

Gaze Stabilization by Efference Copy Signaling without Sensory Feedback during Vertebrate Locomotion

François M. Lambert,^{1,4} Denis Combes,^{2,4} John Simmers,^{2,5,*} and Hans Straka^{3,5,*}

¹Centre d'Etudes de la Sensorimotricité, CNRS UMR 8194, Université Paris Descartes, 45 rue des Saints-Pères, 75006 Paris, France

²Institut de Neurosciences Cognitives et Intégratives d'Aquitaine, CNRS UMR 5287, Université Bordeaux, 146 rue Léo Saignat, 33076 Bordeaux, France

³Biocenter-Martinsried, Department II, Faculty of Biology, Ludwig Maximilians Universität Munich, Grosshadernerstr. 2, 82152 Planegg, Germany

Summary

Background: Self-generated body movements require compensatory eye and head adjustments in order to avoid perturbation of visual information processing. Retinal image stabilization is traditionally ascribed to the transformation of visuovestibular signals into appropriate extraocular motor commands for compensatory ocular movements. During locomotion, however, intrinsic “efference copies” of the motor commands deriving from spinal central pattern generator (CPG) activity potentially offer a reliable and rapid mechanism for image stabilization, in addition to the slower contribution of movement-encoding sensory inputs.

Results: Using a variety of in vitro and in vivo preparations of *Xenopus* tadpoles, we demonstrate that spinal locomotor CPG-derived efference copies do indeed produce effective conjugate eye movements that counteract oppositely directed horizontal head displacements during undulatory tail-based locomotion. The efference copy transmission, by which the extraocular motor system becomes functionally appropriated to the spinal cord, is mediated by direct ascending pathways. Although the impact of the CPG feedforward commands matches the spatio-temporal specificity of classical vestibulo-ocular responses, the two fundamentally different signals do not contribute collectively to image stabilization during swimming. Instead, when the CPG is active, horizontal vestibulo-ocular reflexes resulting from head movements are selectively suppressed.

Conclusions: These results therefore challenge our traditional understanding of how animals offset the disruptive effects of propulsive body movements on visual processing. Specifically, our finding that predictive efference copies of intrinsic, rhythmic neural signals produced by the locomotor CPG supersede, rather than supplement, reactive vestibulo-ocular reflexes in order to drive image-stabilizing eye adjustments during larval frog swimming, represents a hitherto unreported mechanism for vertebrate ocular motor control.

Introduction

Continuous accurate perception of the visual world is an important behavioral requirement during self-generated

motion such as occurs when running, swimming, or flying. All animals are confronted with the disruptive effects of locomotor actions on their ability to perceive the surrounding environment [1], because the consequences of self-motion include head movement that causes retinal image displacement with a resultant degradation of visual information processing. In order to stabilize gaze and maintain visual acuity during locomotion, retinal image drift is minimized by dynamic counteractive eye and/or head-adjustments that in vertebrates are classically attributed to the concerted action of visuovestibular and proprioceptive reflexes [2].

However, earlier behavioral studies in fish suggested that signals other than those arising from these sensory systems might contribute significantly to gaze-stabilizing ocular movements during swimming [3–5]. Moreover, more recent in vitro evidence from larval frogs has suggested that the unidentified eye-adjusting commands during locomotion may in fact originate intrinsically, involving a feedforward representation of the spinal central pattern generator (CPG) output signals that drive actual propulsive body movements [6, 7]. Although such efference copy signaling offers a potentially amenable mechanism for supplementing sensory feedback in counteracting the disruptive visual consequences of self-motion, the underlying neural circuitry as well as the functional relevance of locomotor-extraocular motor coupling and its relationship with movement-encoding sensory signaling remain unknown.

Here, we provide direct evidence that spinal locomotor efference copies do indeed drive effective gaze-stabilizing eye movements during locomotion in larval *Xenopus laevis*. The CPG commands, which arise in the rostral spinal cord, are preferentially targeted to horizontal extraocular motoneurons, consistent with the normal plane of head rotations during tadpole tail-based swimming. These ascending copies of spinal output are relayed directly to their extraocular motor targets, rather than first being integrated with movement-encoding sensory inputs. Importantly, our findings indicate that horizontal vestibulo-ocular reflexes are actively suppressed during regular swimming, thus pointing to a predominant role for intrinsic efference copy signaling in stabilizing gaze during tadpole locomotion.

Results

Compensatory Eye Movements during Real and Fictive Locomotion

Swimming in premetamorphic *Xenopus* larvae is generated by alternating bilateral contractions of myotomal axial muscles that typically produce head-to-tail undulations in the horizontal plane along the animal's body axis [8–10]. As a consequence, left-right head oscillations occur that are accompanied by paired (conjugate) rotations of the eyes in the opposite direction during each half cycle, thereby counteracting the head displacements and stabilizing retinal images (Figure 1A) [6]. These conjugate ocular counterrotations in the horizontal plane are driven by alternate contractions of synergistic pairs of the horizontal lateral rectus (LR) and medial rectus (MR) extraocular muscles [11], which as for vertebrates

⁴These authors contributed equally to this work

⁵These authors contributed equally to this work

*Correspondence: john.simmers@u-bordeaux2.fr (J.S.), straka@lmu.de (H.S.)

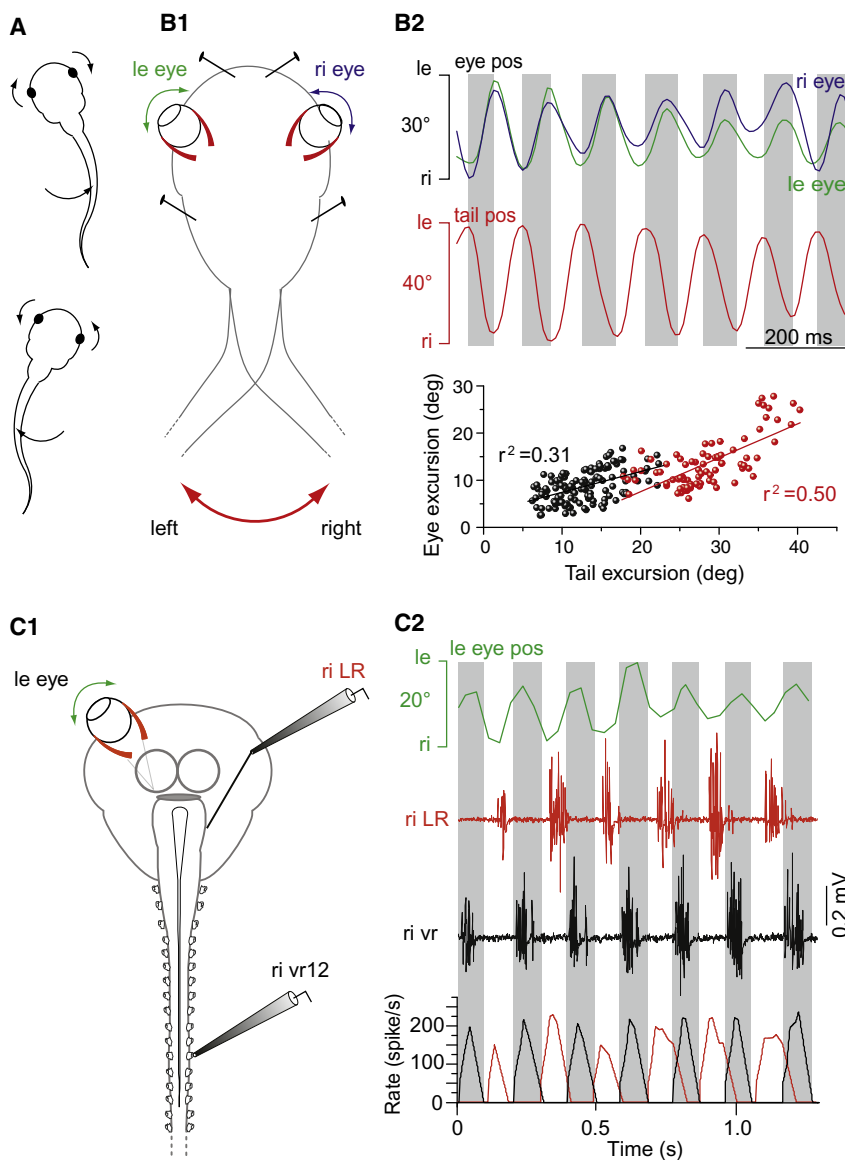


Figure 1. Gaze-Stabilizing Eye Movements and Underlying Extraocular Motor Activity during Real and Fictive Swimming in Stage 55 *Xenopus laevis* Tadpoles

(A) Horizontal head rotations resulting from left-right tail undulations during swimming are associated with oppositely directed, conjugate eye movements.

(B) In a head-fixed animal with a freely moving tail (B1), the left (B2; green trace) and right eyes (blue trace) rotate in phase opposition to spontaneous tail undulations (red trace). The magnitude of eye versus tail excursions (lower plot) in two typical preparations (black and red dots, respectively) during swimming episodes (~40 cycles) indicated an average gain of ~0.6 for compensatory eye motion (see regression slopes with indicated correlation coefficients [r^2]). Note that all semicircular canals and otolith organs had been removed and the optic nerves were cut.

(C1) Schematic of a head-fixed preparation with an intact (left) eye and otherwise isolated brainstem and spinal cord.

(C2) Simultaneous recordings of eye movements along with the multi-unit activity in the right lateral rectus (LR) nerve and right spinal ventral root (vr) 12 during fictive swimming. The lower traces are the corresponding instantaneous nerve firing rates during the displayed cycles. Leftward excursions of the left eye (green) were in phase with burst discharge in the right vr (black) during each cycle of fictive swimming. Rightward eye excursions were in phase with burst firing in the right LR nerve, compatible with conjugate movements of the two eyes.

in general [12], are ascribed to sensory-motor transformations in the hindbrain vestibular nuclei [2].

To assess the extent to which intrinsic feedforward, rather than sensory feedback, signals might also contribute to the gaze-stabilizing process [6], we made high-speed video recordings of eye and undulatory tail movements during swimming in animals with their heads held stationary and following bilateral removal of the labyrinthine endorgans and transection of both optic nerves. In such head-fixed, tail-free preparations (Figure 1B1), swimming-related eye movements continued to occur, which were therefore produced independently of any head displacement and optokinetic responses (Figure 1B2). Moreover the conjugate eye rotations were oppositely directed to the spontaneous tail undulations and had cycle-by-cycle amplitudes that were proportional (gain ~0.55; $n = 5$) to the magnitude of tail excursion. This functional relationship observed in vivo in the absence of both angular head acceleration and visual inputs therefore confirmed that neural signals other than those arising from the sensing of head and/or retinal image motion make a behaviorally relevant

contribution to counteractive ocular movements in the swimming tadpole.

Neural correlates of this tail-eye movement coordination was also expressed in reduced preparations in which the body and tail musculature was removed and the extraocular muscle innervation of one eye was severed for recording from the peripheral end of the severed stumps, whereas the contralateral eye and its motor nerves remained intact (Figure 1C1). So-called “fictive swimming” (frequency 6.2 ± 0.26 Hz; $n = 24$) expressed spontaneously by such preparations consisted of rhythmic spinal ventral root (vr) bursts that would normally drive muscle contractions underlying left-right tail undulations in vivo (Figure 1C2) [6, 10]. Moreover, movements of the still intact (left) eye remained coordinated with (right) spinal vr discharge in a temporal relationship that would be oppositely directed to actual tail bending (see Figure 1A). Correspondingly, the LR motor nerve of the right eye displayed rhythmic bursting that was coordinated with spinal motor bursts during fictive swimming (Figure 1C2). Again, the timing of this extraocular nerve activity was appropriate for producing horizontal eye movements that would oppose head oscillations and minimize retinal image slip during real behavior.

Spinal Origin of the Locomotor Efference Copy

In principle, the locomotor-related drive to extraocular motoneurons could originate at a supraspinal level, such as the midbrain centers known to control locomotor behavior [13].

Spinal Efference Copy Control of Eye Movements

3

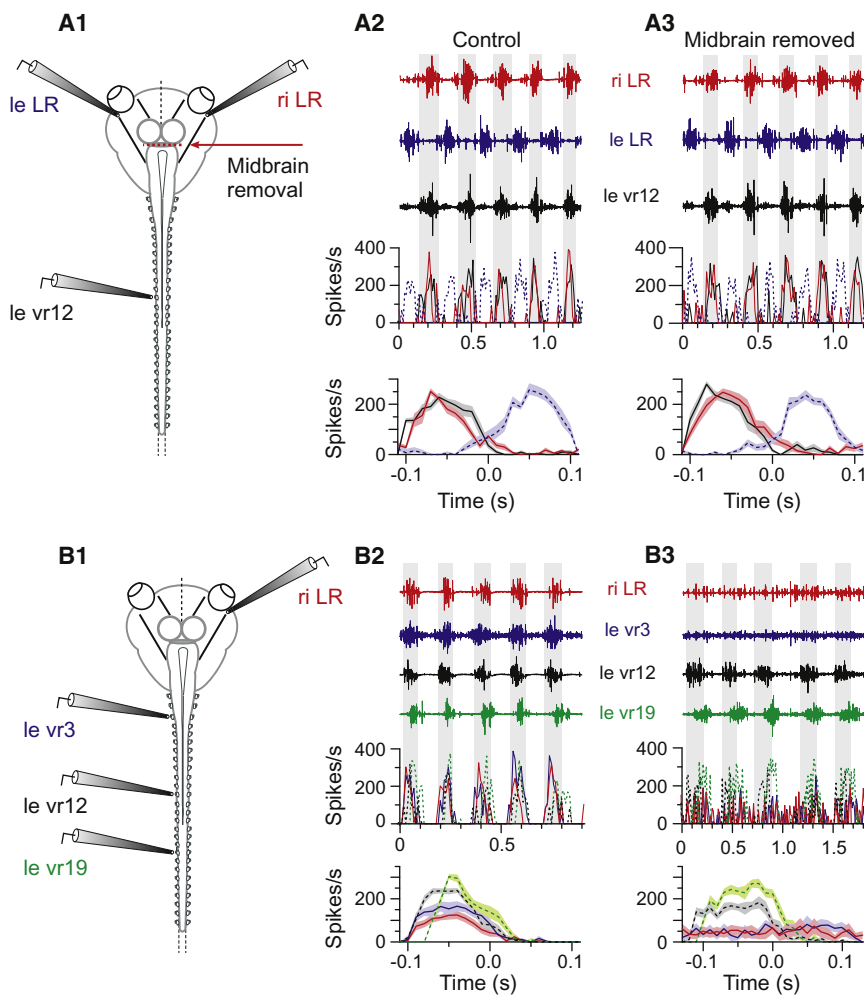


Figure 2. Spinal Cord Origin of Locomotor Related Extraocular Nerve Activity

(A1 and B1) In vitro brainstem-spinal cord preparations depicting recording protocols. (A2 and A3) Coordinated rhythmic bursting in spinal vr 12 (black) and left (blue) and right (red) LR motor nerves (A2) remained unaffected by removal of the midbrain (A3). Lower panels in (A2) and (A3) show corresponding impulse firing rates during the five displayed cycles, and mean discharge rates (\pm SEM, shaded area in each plot) over a single locomotor cycle averaged from 25 consecutive cycles. (B2 and B3) Bursting in the right LR motor nerve (red) coupled with bursts in different segments along the left side of the cord (B2; vr3, blue; vr12, black; vr19, green), disappeared (B3) when locomotor CPG activity ceased spontaneously in rostral vr3 but persisted in caudal vr12 and vr19. Same figure layout as in (A2) and (A3).

Target Specificity of Spinoextraocular Coupling

During fictive swimming, the mean multiunit firing rate in the LR nerve increased cyclically by \sim 6-fold (Table S1), coincident with locomotor bursts on the opposite side of the cord (Figures S2A1 and S2A2). Similarly, discharge in the ipsilateral MR nerve increased by \sim 7-fold in bursts that were now in phase with vr output on the same cord side (Figures S2A1 and S2A3). The activation profiles and their timing in these antagonistic extraocular motor nerves were therefore appropriate for driving muscle contractions that produce alternate right-left eye

rotations during each swim cycle, in antiphase with rostral trunk movements.

However, this possibility was excluded by removing the midbrain from completely isolated brainstem and spinal cord preparations (Figure 2A1; $n = 5$) in which the rhythmic activation of extraocular motoneurons during fictive swimming persisted in the absence of all movement-derived sensory feedback (see Figure S1A available online). Neither the magnitude of the locomotor-timed discharge in the LR and spinal motor nerves nor their phase relationships were affected by a midbrain ablation (Figures 2A2 and 2A3), indicating that the locomotor feedforward signals to the extraocular motor nuclei originated from the spinal CPG itself.

The spinal source of the locomotor-timed influence on extraocular motor output was further substantiated by recording vr activity at different segmental levels along the in vitro spinal cord during bouts of fictive swimming (Figure 2B1; $n = 10$). As seen in Figure 2B2, robust cyclic discharge in a LR nerve was phase-coupled with rhythmic bursts that were uniformly expressed in the contralateral vrs along the cord. However, the spino-extraocular coupling disappeared in all preparations ($n = 10$) whenever bursting in the most rostral vrs (segments 1–10) occasionally ceased, although bursting persisted in more caudal roots (Figure 2B3; Figure S1B). These findings therefore support the conclusion that the signals for locomotor-extraocular coupling arise principally from rhythmically active CPG circuitry in the anterior cord region.

The firing patterns of LR and MR motoneurons during fictive swimming closely matched the discharge profiles of vestibulo-ocular reflexes (VORs). In semi-intact preparations with functional vestibular endorgans, imposed vertical-axis sinusoidal rotations (1 Hz) (Figure S2B1) caused LR nerve firing rates to increase during head motion directed contralaterally to the recorded nerve (contraversive) and decrease during (ipsiversive) movement toward the same side (Figure S2B2; Table S1). A similar discharge modulation, but now in phase-opposition, was observed in the ipsilateral MR nerve (Figure S2B3), where firing increased during ipsiversive and decreased during contraversive passive head rotations (Table S1). These nerve responses thus corresponded to the classical horizontal semicircular canal-driven VOR, which is considered to be the major contributor to minimizing retinal image slip during angular head rotation [2, 11, 14].

In contrast to the strong modulation of LR and MR nerve discharge during fictive swimming (Figures S2A2 and S2A3), motor pools that innervate vertical or oblique eye muscles were only weakly modulated or remained unaffected by spinal CPG activity (Figures S2A4 and S2A5). Again, the limited CPG influence on these extraocular motor pools matched their weak responsiveness to horizontal semicircular canal stimulation by passive, vertical-axis head rotations (Figures S2B4

rotations during each swim cycle, in antiphase with rostral trunk movements.

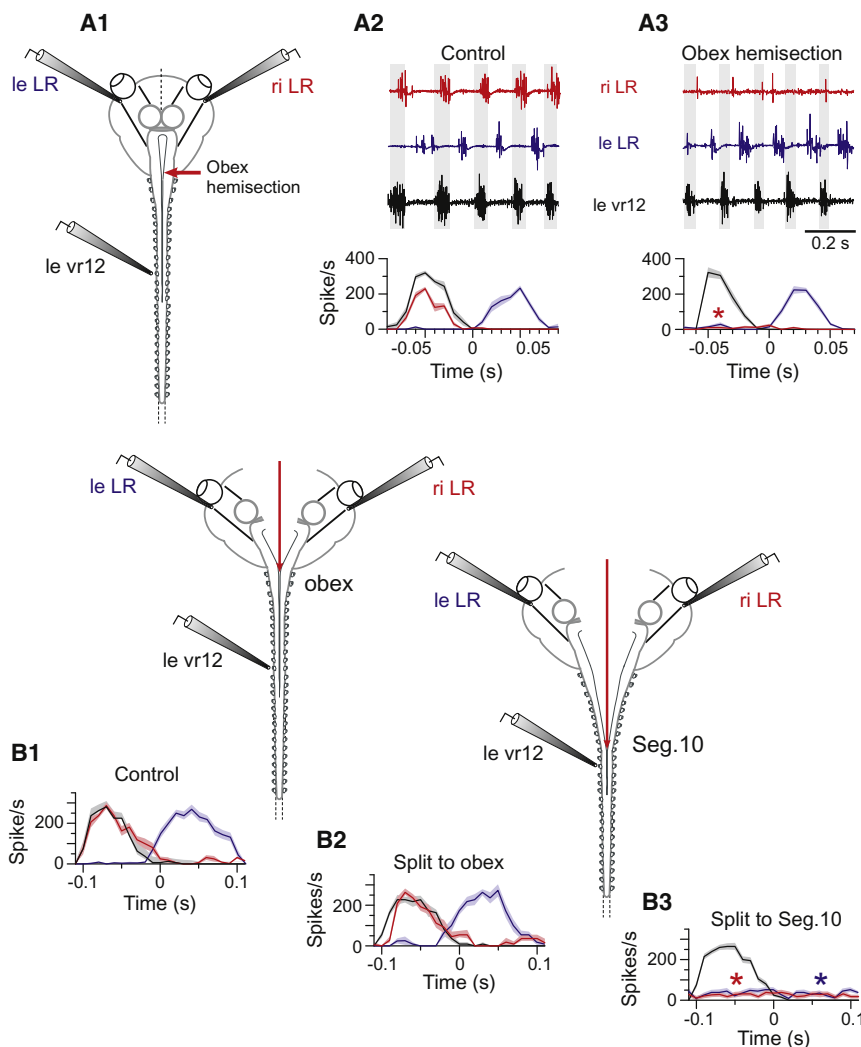


Figure 3. Trajectory of Ascending Pathway from Locomotor CPG Circuitry in the Rostral Spinal Cord to LR Motoneurons in the Brainstem

(A1) Isolated CNS preparation and recording protocol. Spinoextraocular coupling during fictive swimming (A2) monitored in left vr12 (black) was suppressed in the right (red) but not the left (blue) LR (A3) by a right cord hemisection at the obex (at red arrow in A1); lower plots in (A2) and (A3) show mean firing rates (\pm SEM, shaded area in each plot) over a single cycle in the left vr (black), right LR (red), and left LR (blue) averaged from 15 consecutive burst cycles.

(B) In a different preparation, a longitudinal midline split of the brainstem until the obex did not disrupt spinoextraocular coupling in either LR (B1 and B2), whereas an extended sagittal separation until cord segment 10 (B3) caused a complete loss of spino-LR coupling, without affecting ongoing locomotor bursting in more caudal vr12. Plots in the three experimental conditions in (B) show discharge rates over a single cycle for the left vr12 (black), left LR (blue), and right LR (red) averaged from 24 fictive swim cycles.

and right LR nerve, for example (Figure 3B1; $n = 6$), remained unaffected by a midline separation of the entire brainstem as far as the obex (Figure 3B2). However, when this sagittal lesion was extended until spinal segment 10, the CPG drive to both the left and right LR motor nerves disappeared (Figure 3B3; $n = 8$; see also Figure S1C), thereby indicating that the contralateral ascending pathway originates in the rostral cord region.

On reaching the brainstem, the locomotor signals could be conveyed directly to their extraocular motor targets. Alternatively, the efference copy could be first integrated with sensory inputs in the vestibular nuclei before being relayed to LR motoneurons in the abducens motor nucleus via established vestibulo-ocular pathways [11]. Several lines of evidence strongly supported the former and excluded the latter possibility. First, in semi-isolated preparations with functional labyrinthine endorgans, a unilateral pressure-injected mixture of CNQX and 7CI-KYNA (both 100 μ M) into the vestibular nuclei (Figure 4A1; $n = 5$) to block glutamatergic transmission between labyrinthine afferents and second-order vestibular neurons [16], suppressed the activation of LR motoneurons by passive head rotation (Figure 4A2), without affecting the spinal drive to these neurons during subsequent fictive swimming (Figure 4A3). This persistence of CPG coupling despite VOR blockade thus indicated that vestibular nuclear circuitry was not interposed in the efference copy pathway. Second, a unilateral electrical stimulation of the ventral spinal cord near the obex evoked impulses in the ipsilateral LR nerve with a relatively brief (~ 3 ms) and constant delay (Figure 4B; $n = 6$), compatible with underlying mono- rather than disynaptic connectivity. Third, direct access of the spinal pathways to LR motoneurons was supported by anatomical evidence. Application of Alexa Fluor 488 dextran crystals to the abducens nucleus (Figure 4C1; $n = 6$)

and S2B5), in accordance with the general spatial organization of VOR sensory-motor connectivity [15]. These data therefore indicated not only that eye counter rotations can be driven by two separate commands, one sensory and the other central and motor in origin, but also that the horizontal plane-specificity of both signals corresponded to the movement dynamics of normal swimming behavior.

Pathway Trajectory of Efference Copy Signals to LR Motoneurons

To locate the neural pathways that mediate spinoextraocular motor coupling, we made a series of specific lesions in vitro preparations generating locomotor activity spontaneously. A right-side hemisection of the cord just caudal to the obex (Figure 3A1) suppressed CPG-driven bursts in the right LR nerve (Figure 3A3; $n = 8$), which in the intact CNS occurred in phase with vr bursts on the left side of the cord (Figure 3A2). However, the spinal drive to left LR motoneurons (i.e., contralateral to the lesion) remained unaffected both in magnitude and timing (Figures 3A2 and 3A3). These initial findings therefore indicated that the pathway linking each side of the cord to the contralateral LR motor pool involves ascending axons that cross the midline below the obex. In confirmation of this trajectory, the diagonal in-phase coordination between the left vr12

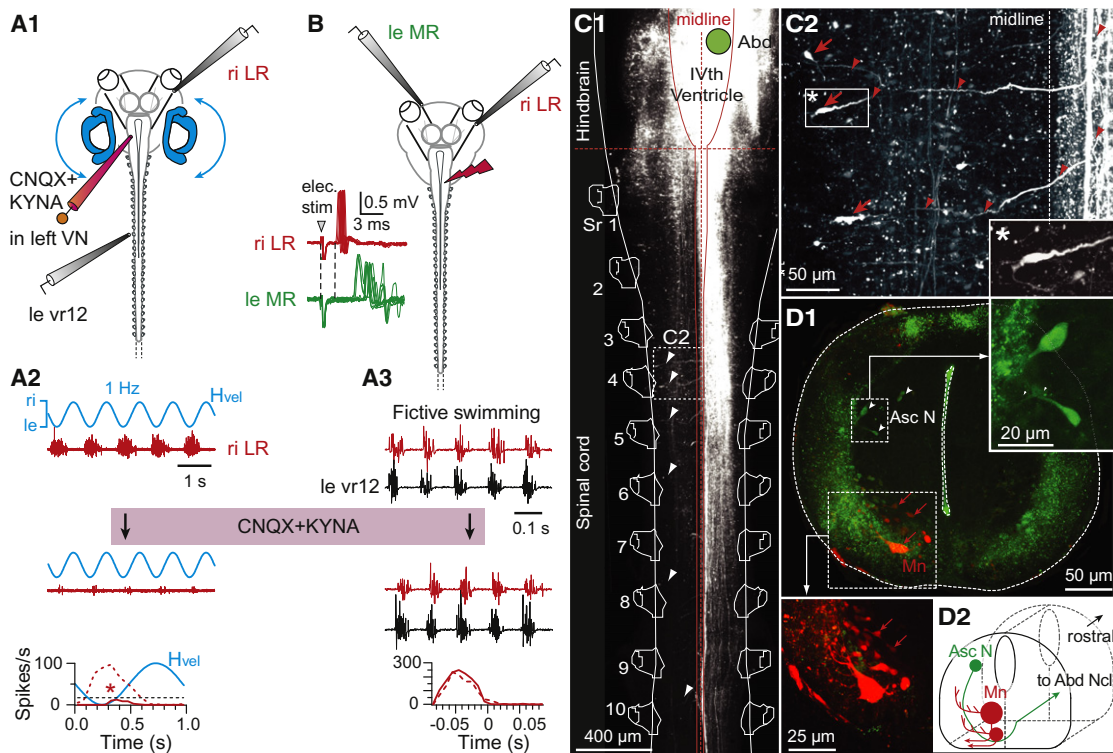


Figure 4. Physiological and Anatomical Evidence for a Direct Ascending Pathway from Rostral Cord Segments to LR Motoneurons in the Abducens Nucleus (A1) Experimental protocol for (A2) and (A3). Burst activity in the right LR nerve (red) evoked by vertical axis rotation at 1 Hz and $\pm 60^\circ/s$ (A2, upper panel) was blocked by focal pressure injection of 100 μ M CNQX and 100 μ M 7Cl-KYNA into the left vestibular nuclei (A2, lower panel), but spinoextraocular coupling seen during a subsequent episode of fictive swimming (A3, upper panel) remained unaffected (A3, lower panel). Plots in (A2) and (A3) are averaged LR firing rates before (dashed red lines) and after (solid red lines) drug application in the two experimental conditions.

(B) Single pulse electrical stimulation to one side of the ventral cord surface at the obex evoked short-latency spike discharge in ipsilateral LR motoneurons (red) and longer-latency firing in contralateral MR motoneurons (green). The traces are an overlay of eight individual responses.

(C) Photomicrographs of a whole mount (C1) and amplified view (C2, from boxed area in C1) of retrogradely labeled axons (red arrowheads in C2) and cell bodies (red arrows and inset * in C2) in the lateral margin of the left rostral spinal cord after application of Alexa Fluor 488 dextran to the right abducens nucleus (green circle in C1).

(D1) Coronal section showing green stained somata of contralaterally ascending spinal neurons (Asc N; white arrow heads) in the dorsal marginal zone along with ventrally located axial motoneurons (Mn; stained red) after back-filling with Alexa Fluor 546 dextran from the corresponding ventral root.

(D2) Summary schematic of a contralaterally ascending spinal neuron (green Asc N) in relation to spinal motoneuron (red Mn) location.

consistently labeled a small population of ~ 50 spinal neurons with relatively small, segmentally iterated somata located contralateral to their rostrally projecting axons (Figures 4C1 and 4C2). Moreover, in correspondence with our physiological data (e.g., Figures 2B3 and 3B3; Figures S1B and S1C), these ascending neurons were distributed in the first ten spinal segments. In contrast to ventrally positioned motoneurons, their somata lie in the dorsolateral cord marginal zone (Figures 4D1 and 4D2). Their axons then project ventrally beneath the canal to cross the midline in the segment of origin before projecting rostrally in distinct ventromedial fiber bundles to the abducens nucleus (Figures 4C1, 4C2, and 4D2).

Efference Copy Signaling to MR Motoneurons

Although the left and right MR motor pools are each coactive with ipsilateral spinal vrs during fictive swimming (Figure 5A, upper plot), their coupling was also interrupted solely by a cord hemisection made at the obex on the opposite side (Figure 5A, lower plot; $n = 6$). This lesion therefore indicated that spinal-MR coupling does not involve separate homolateral ascending projections. Rather, spinal signals are initially conveyed in the contralateral cord as for synergistic LR

motoneurons but subsequently must retrace the midline in the brainstem.

Two lines of evidence suggested that this second cross-over occurs at the level of the abducens nucleus, at the site where the first-order spinal projections reach their LR motor targets. First, a restricted sagittal midline incision in rhombomere 5 (r5) where the abducens nucleus is located [17], suppressed the spinal CPG drive to MR motoneurons on both sides (Figure 5B; $n = 6$), without affecting spino-LR motor coupling. Second, blocking glutamatergic synapses in the right abducens nucleus with focally injected CNQX/KYNA (Figure 5C1; $n = 5$) suppressed passive head rotation-evoked activity in the left MR nerve (Figure 5C2), as well as CPG-driven bursts during fictive swimming (Figure 5C3). In contrast, both VOR- and CPG-derived activation of LR motoneurons on the left, noninjected side remained unaffected (Figures 5C2 and 5C3). These findings therefore supported the conclusion that the recrossing access to MR motoneurons in the brainstem occurs through a second-order, synaptically activated pathway that originates in the abducens nucleus. Interestingly, abducens internuclear neurons (Abd In; Figure 5D), whose axons traverse the

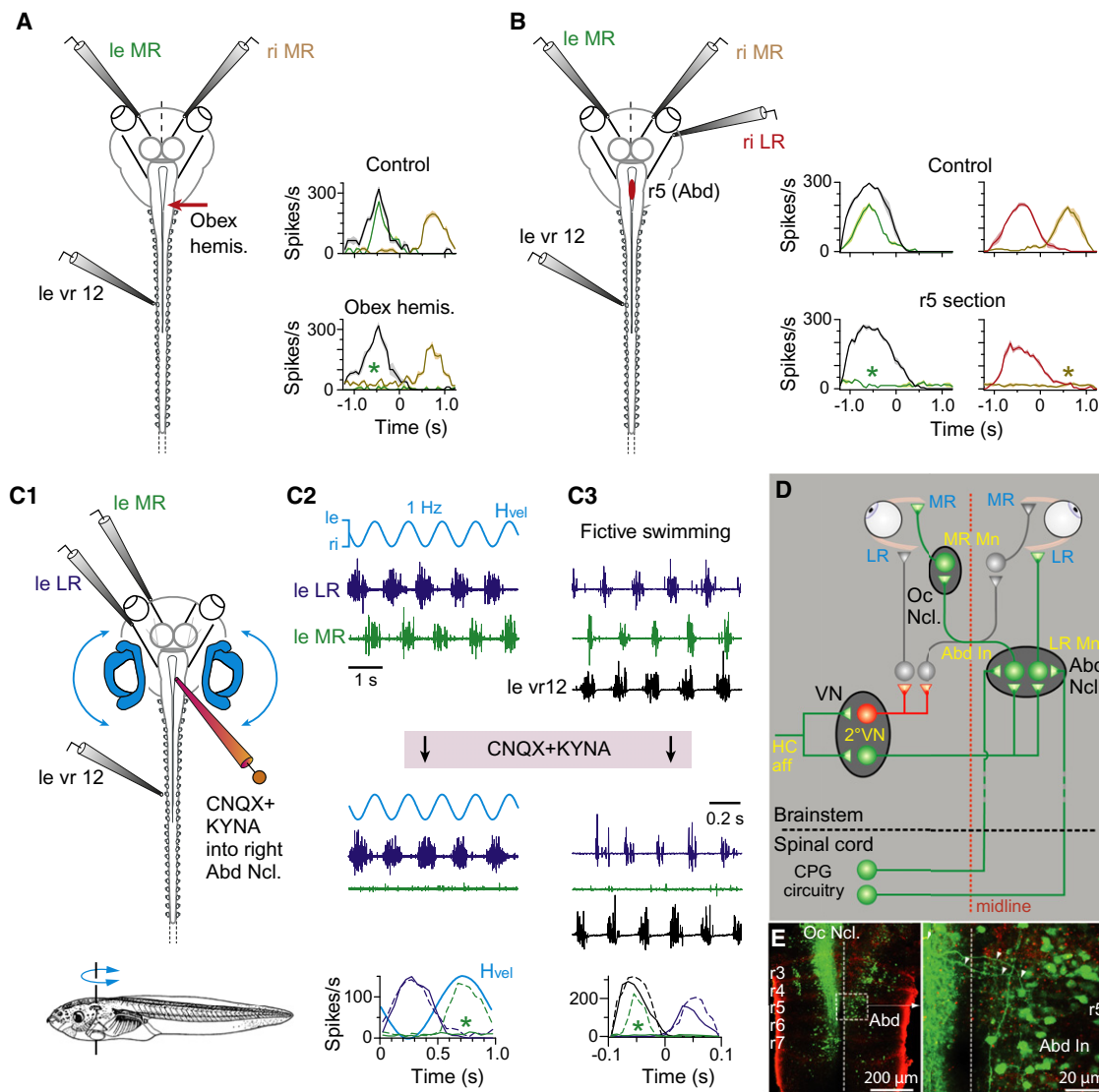


Figure 5. Pathway Trajectory from the Spinal CPG to MR Motoneurons in the Oculomotor Nuclei

(A and B) Experimental protocols (left) and plots of mean discharge rates (± SEM, shaded area in each plot) over one cycle for a left spinal vr (black traces), left (green) and right (gold) MRs, and a right LR (red) averaged from 15 consecutive cycles of fictive swimming.

(A) Burst coordination with left vr12 disappeared in the left but not the right MR after a right-side cord hemisection (red arrow in schematic) at the obex. (B) A short midline incision in the abducens nucleus at rhombomere 5 (r5) suppressed spinoextraocular coupling in both MRs (green and gold plots) but not in the right LR nerve (red plot).

(C) Blockade of glutamatergic synaptic transmission in an abducens nucleus suppressed both passive head rotation- and spinal CPG-driven extraocular activity. Pressure injection of CNQX and 7Cl-KYNA (both 100 μM) into the right abducens nucleus (C1) blocked left MR (green) activation by passive vertical-axis head rotations at 1 Hz and ± 60°/s (C2) and during fictive swimming (C3), whereas left LR (blue) responses remained unaffected in both situations (see average firing rate plots in lower C2 and C3; solid and dashed lines represent conditions before and after CNQX + KYNA, respectively).

(D) Summary schematic of vestibular afferent circuitry, ascending spinoabducens pathways and abducens-oculomotor connectivity via abducens internuclear neurons (Abd In).

(E) Origin of Abd In. in the right Abd Ncl. of r5 after retrograde labeling with Alexa Fluor 488 dextran (green) from the left oculomotor nucleus (Oc Ncl.). The midline-crossing axons and cell bodies of Abd In. (white arrow heads) are seen in greater detail in the magnified view at right.

midline in r5 (Figure 5E), serve to couple synergistic LR and MR motoneurons on opposite sides to produce conjugate eye movements during the horizontal VOR [11]. It is therefore likely that these diagonally projecting cells are also responsible for relaying spinal efference copy signals to MR motoneurons upon the formers' arrival in the abducens nucleus. The ~6 ms latency to MR motoneuron activation in response to a stimulation at the obex (Figure 4B) is also consistent with such a disynaptic pathway [11].

Efference Copy Interactions with Sensory Feedback Signaling

How might reflexive vestibular signals and intrinsic locomotor commands cooperate to stabilize gaze in the swimming tadpole? Given the similar spatiotemporal specificities of horizontal semicircular canal feedback and CPG feedforward influences (Figure S2), a reasonable first assumption was that the two signals combine to enhance the gain and precision of extraocular motor responsiveness [6]. To test this prediction,

Spinal Efference Copy Control of Eye Movements

7

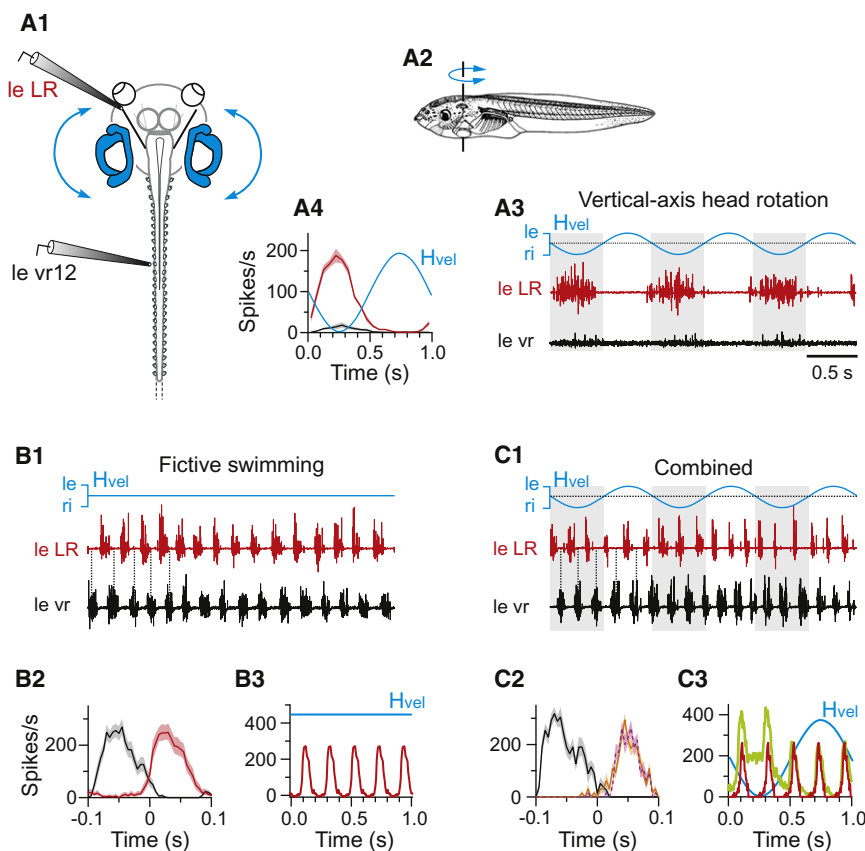


Figure 6. Suppressive Interaction between Spinal Locomotory Efference Copy and Horizontal Semicircular Canal-Activated VOR

(A1 and A2) In vitro preparation with intact vestibular sense organs (A1) subjected to passive vertical-axis head rotations (blue arrow in A2).

(A3) Left LR (red) and vr12 activity (black) evoked by sinusoidal head rotations at 1 Hz and $\pm 60^\circ/\text{s}$ (blue, H_{vel}).

(A4) Averaged discharge rates (\pm SEM, shaded area in each plot) of le LR and le vr12 (n = 50) during one cycle with respect to H_{vel}.

(B and C) In the same preparation, spinoextraocular coupling and corresponding mean discharge rates (B2 and C2; le vr, black; le LR, red plots) during spontaneous fictive swimming in the absence (B1 and B2) and additional presence (C1 and C2) of vertical-axis head rotations as in A3. The overlaying orange and violet plots in C2 represent separate mean LR discharge rates during the rightward (gray shaded areas in C1) and leftward phases (unshaded areas in C1) of table rotation.

(B3) Average LR firing rate modulation over five fictive swim cycles.

(C3) Arithmetic summation (green) of passive head acceleration-evoked LR activity (A4) and spinal CPG-driven bursts (B3). The red trace in C3 is the actual LR firing rate modulation over five fictive swim cycles during concomitant vertical-axis rotation (colored plots in C2) indicating cancellation of horizontal canal input.

we conducted experiments on semi-isolated preparations with intact labyrinths (Figure 6A1; n = 8) that were subjected to vestibular afferent activation in the absence of, or in combination with, spontaneous fictive swimming. Vertical axis head rotations (Figure 6A2) applied at 1 Hz caused a strong modulation of LR nerve firing in a phase relationship that was typical for the horizontal angular VOR (aVOR) (Figures 6A3 and 6A4) [11]. In the same preparation, but without passive head movement, spontaneous fictive swimming elicited rhythmic LR nerve bursts (Figures 6B1–6B3) that were also appropriately timed for producing ocular counterrotations to active head displacement in the intact animal. In a crucial third step, LR motor nerve responses were observed when spinal CPG activity now occurred during ongoing turntable rotations (Figures 6C1 and 6C2). Surprisingly, in this combined condition, LR motoneuron bursts continued to be expressed in strict coordination with fictive locomotion (Figures 6C1, cf. 6B1), whereas any VOR-mediated sensory feedback influence on LR firing disappeared (Figures 6C1, cf. 6A3).

The loss of the horizontal aVOR during fictive swimming was further verified by comparing the firing rates within CPG-driven LR bursts during the two directional phases of vertical-axis rotation. Whereas during passive head rotations alone, when LR motoneurons were activated during contraversive and inhibited during ipsiversive motion (Figure 6A3; shaded and unshaded areas, respectively), in the combined condition (Figure 6C1), the locomotor-timed LR bursts had identical discharge profiles irrespective of the phase of imposed movement (Figure 6C2). The close similarity between LR bursts occurring during fictive swimming alone (Figure 6B3) and those expressed during concurrent head rotations (Figure 6C3, red trace), in contrast to the theoretical waveform produced by

artificially combining the two independent responses (Figure 6C3, green trace), thus confirmed the complete lack of any additive relationship between semicircular canal inputs and spinal efference copies. Rather, during locomotor rhythmogenesis, access of these vestibular afferent signals to extraocular motoneurons appeared to be actively suppressed.

The sensory feedback cancellation during locomotor activity might be specific to inputs arising from the horizontal semicircular canals, or it may represent a general inhibitory action on vestibulo-ocular reflexes. We therefore examined spinoextraocular motor coupling during spontaneous fictive swimming and passive head rotations that activated vestibular endorgans other than the horizontal semicircular canals (Figures 7A1 and 7A2). In otherwise quiescent preparations (n = 6), imposed left-right head rolling caused a strong modulation of LR nerve firing that increased and decreased during contraversive and ipsiversive movements, respectively (Figures 7A3 and 7A4), in accordance with the directional specificity of the VOR in this plane [18, 19]. Moreover, because LR nerve discharge was similarly modulated at both high and low velocities and/or frequencies (data not shown), the motor responses arose mainly from a gravito-inertial activation of utricular inputs [14].

In the same preparations, spontaneous fictive swimming in the absence of head-roll stimulation also elicited rhythmic LR nerve bursts (Figures 7B1–7B3), as seen previously (Figures 6B1–6B3). However, during locomotor activity in conjunction with passive roll movements (Figure 7C1), the firing pattern expressed by LR motoneurons now resembled a combination of the patterns occurring in the two separate experimental conditions (cf. Figures 7A3 and 7B1). This additive LR responsiveness to efference copy and vestibular sensory afferent

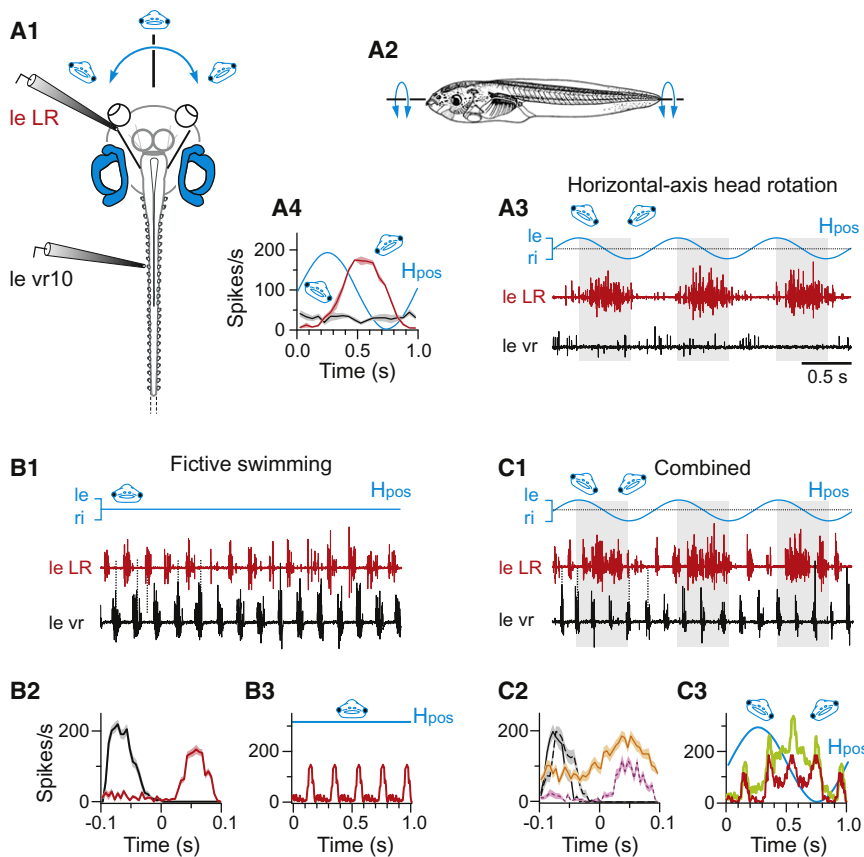


Figure 7. Combinative Interaction between Spinal Locomotor Efference Copy and Head Roll-Activated VOR

(A1 and A2) In vitro preparation (A1) subjected to horizontal-axis rotations (blue arrow in A2). (A3) Left LR (red) and vr12 activity (black) evoked by sinusoidal head tilting at 1 Hz and $\pm 60^\circ$ (blue, H_{vel}). (A4) Averaged discharge rates (\pm SEM, shaded area in each plot) of le LR and le vr12 ($n = 45$) plotted during one cycle with respect to H_{vel} . (B and C) In the same preparation, spinoextraocular coupling and corresponding mean discharge rates (B2 and C2; le vr, black; le LR, colored plots) during spontaneous fictive swimming in the absence (B1 and B2) and additional presence (C1 and C2) of horizontal-axis rotations as in (A3). The orange and violet plots in (C2) represent separate mean LR discharge rates during left-side down (gray shaded areas in C1) and right-side down (unshaded areas in C1) head tilting. (B3) Average LR firing rate modulation over five fictive swim cycles. (C3) Arithmetic summation (green) of head tilting-evoked LR activity (A4) and spinal CPG-driven bursts (B3). The red trace in (C3) is the actual LR firing rate modulation over five fictive swim cycles during concomitant horizontal-axis rotation (colored plots in C2) indicating an additive responsiveness to efference copy and vestibular sensory input. Note that the actual discharge levels in the LR remained lower than the peak frequencies of the theoretical profile, probably due to a rate-limiting saturation of neuronal firing mechanisms.

influences was further indicated by comparing the extraocular nerve's CPG-driven discharge profiles during the alternate phases of imposed head displacement (Figures 7A3 and 7C1). Both the peak and trough intensities of LR firing during each contraversive head roll movement were significantly enhanced relative to the nerve's activity during the ipsiversive phase of head movement (Figure 7C2). Moreover, the intensity of spinal vr bursts themselves remained unaltered throughout the two movement phases, indicating that the roll-induced modulation of LR firing was not somehow due to vestibular-driven fluctuations in the strength of ongoing CPG activity. Thus, in the combined experimental situation, the LR discharge profile over each movement cycle (Figure 7C3, red trace) approximated that obtained theoretically by summing the actual LR responses to independent head-roll (Figure 7A4) with those from spinal CPG (Figure 7B3) activation (Figure 7C3, green trace).

Together, these data therefore provide compelling evidence that in *Xenopus* tadpoles, the convergence of locomotor efference copies with head movement-related vestibular sensory signals does not involve a generalized additive process in extraocular motor control. Rather, whereas sensory motor transformations of vestibular inputs compensate for passive displacements of the head in space, according to plane specificity, these ocular motor reflexes may be either supplemented or totally supplanted by predictive spinal (extravestibular) commands during self-motion.

Discussion

Here, we have established that spinal CPG efference copies in *Xenopus* tadpoles ensure visual field-stabilization by driving

eye movements appropriate to counteract rotational head displacements during undulatory swimming. The intrinsic CPG signals are conveyed by direct diagonal pathways from the rostral spinal cord to contralateral LR motoneurons and in turn via abducens internuclear neurons to synergistic MR motoneurons in the contralateral oculomotor nucleus. The spatial specificity and functional impact of these extravestibular signals on extraocular motoneurons match those of the sensory-driven horizontal aVOR. However, instead of contributing collectively to the image-stabilizing process, during regular swimming behavior that is typically in the horizontal plane, the horizontal aVOR is suppressed and plays no role in counteractive movement. This previously unreported finding therefore challenges our traditional understanding of how animals offset the disruptive effects of self-generated, rhythmic body and head movements on visual processing.

Our initial discovery suggesting that image stabilization during larval *Xenopus* locomotion relies at least in part on spinal efference copy signals was already unexpected [6]. However, the novel additional finding that intrinsic feedforward commands do not act synergistically with horizontal semicircular canal inputs, which together could have been expected to augment the gain of extraocular motor responses, is even more surprising. Rather, the selective suppression of these vestibular feedback signals during stereotyped swimming implies that CPG-derived commands serve as the predominant mechanism for minimizing retinal image slip while the animal is executing locomotor behavior. Importantly, in vivo measurements during actual swimming movements in animals lacking vestibular and visual inputs revealed that the amplitudes of ongoing eye rotations relative to oppositely directed tail undulations had a gain of ~ 0.6 . Thus the

spinal efference drive, which normally would be supplemented by optokinetic reflexes (gain ~ 0.4) [14], is indeed capable of ensuring effective gaze stabilization without vestibular sensory signaling. However, the latter is presumably called into play such as when the animal deviates from its steady rectilinear trajectory in response to external perturbations, during rapid-start escape behavior, or during voluntary postural adjustments during slower swimming or nonlocomotory behavior.

A defining feature of motor efference copy is its provision of rapid, predictive information that preempts the slower engagement of movement sensing pathways and is thereby able to estimate, in both amplitude and timing, the sensory consequences of a behavioral action [20, 21]. During stable undulatory swimming, stage 55 *Xenopus* tadpoles attain cycle frequencies of 5 to >10 Hz [10, 22], corresponding to cycle periods down to the 100 ms range. Accordingly, the ~ 10 ms delay until the onset of VOR-driven extraocular muscle contractions observed during passive head rotation [11] may be too slow for meaningful eye movement control on a rhythmic cycle-by-cycle basis. The speed and temporal precision of inbuilt feedforward signaling may therefore account for its restricted deployment in maintaining visual stability during tadpole locomotion. Although the mechanism(s) by which the horizontal aVOR is selectively gated-out during swimming remains to be determined, it is plausible that blockade is similar to the way in which inappropriate spinal 1a afferent reflexes are suppressed by presynaptic inhibition during walking in terrestrial vertebrates [23, 24]. Interestingly, compensatory eye movements occurring at near zero delay with active postural head rotations and independently of vestibular sensory input have been recently reported in the guinea pig [25], although the neural origin of these anticipatory ocular responses has yet to be identified.

It is also possible that locomotor efference copy signaling in extraocular motor control is representative of an ancestral condition in early vertebrates before the appearance of present day vestibular endorgans. Compatible with this idea is the relatively late evolutionary arrival of horizontal semicircular canals, which only appeared in jaw-bearing vertebrates [26] long after the emergence of undulatory tail-based swimming in their tadpole-like chordate ancestors [27, 28]. Indeed, the considerable delay before the first appearance of horizontal semicircular canals through the founder recruitment of the ancestral gnathostome *Otx* gene [29, 30] might have been attributable to a lack of evolutionary pressure. Until then, effective gaze stabilization could have been adequately accomplished by spinal CPG-driven signals during the tail-based locomotor strategy used by these aquatic vertebrate ancestors, as occurs in some of their present-day protochordate lineages [28, 31]. In the latter groups moreover, the most anterior region of the neuraxis, which bears homologies with the vertebrate hindbrain [32, 33], contains myotomal motor circuitry that extends beyond the spinal cord. In larval *Xenopus*, the presence of linking pathways from rostral cord segments to the hindbrain abducens nucleus is consistent with such an extraspinal relationship, effectively enabling the extraocular motor nuclei to become an extension of, and appropriated to, spinal CPG circuitry during locomotion. In this case, however, the coupling occurs between two otherwise functionally and anatomically distinct motor systems.

The involvement of spinal efference copy in stabilizing gaze during locomotion may be more prevalent in aquatic anamniote vertebrates, including larval amphibians (this study)

[6, 7] and fish [3, 4] than previously suspected. Pertinent to this possibility is the biomechanical rigidity of the head/body coupling in these undulatory swimming animals, with the restricted degrees of freedom imparting relative predictability to the retinal image shifts resulting from the accompanying horizontal head oscillations. However, it is not implausible that spinal efference copy signals also access the brainstem ocular motor control pathways in other vertebrates confronted with more complex visual disturbances resulting from their flexible necks and/or limb-based locomotor strategies.

In this context, supportive evidence both for the presence of spinal efference copy signaling in mammals and its suppressive interaction with vestibular sensing during locomotion is available from clinical studies on the pathological effects of a unilateral vestibular loss [34, 35] and the resulting asymmetric deficits in gaze and posture control [36]. In unilateral vestibulopathic dogs [34] and humans alike [35], postural instability is significantly diminished during running compared to walking, inferring that programmed rhythmic output from the spinal locomotor generator [37] reduces destabilizing tonic vestibular inputs during faster, more autonomous self-motion. Similarly, perturbation of vestibular signaling by galvanic labyrinthine stimulation in normal human subjects causes smaller trajectory deviations during running than walking [38], again compatible with an activity-dependent, CPG-derived gating of vestibular sensory influences. It is therefore likely that a negative relationship between internal feedforward commands and afferent feedback signaling, and the hitherto unestablished implications for gaze control during locomotion are not confined to the simpler amphibian tadpole.

Experimental Procedures

Experiments were conducted on larval *Xenopus laevis* at stage 55 [39] in compliance with the "Principles of Animal Care," publication No. 86-23 (revised 1985) by the National Institutes of Health. In vitro electrophysiology, pharmacology, anatomy, lesioning, and behavioral methods are detailed in the [Supplemental Information](#).

Supplemental Information

Supplemental Information includes two figures, one table, and Supplemental Experimental Procedures and can be found with this article online at <http://dx.doi.org/10.1016/j.cub.2012.07.019>.

Acknowledgments

This research was supported by the French "Agence Nationale de la Recherche" (ANR-08-BLAN-0145-01) and by the German Science Foundation (SFB 870, B12). The authors are grateful to Tobias Kohl and Anne Le Seach for help with analysis programs.

Received: June 1, 2012

Revised: July 6, 2012

Accepted: July 6, 2012

Published online: July 26, 2012

References

1. Cullen, K.E. (2004). Sensory signals during active versus passive movement. *Curr. Opin. Neurobiol.* 14, 698–706.
2. Angelaki, D.E., and Hess, B.J. (2005). Self-motion-induced eye movements: effects on visual acuity and navigation. *Nat. Rev. Neurosci.* 6, 966–976.
3. Easter, S.S., Jr., and John, P.R. (1974). Horizontal compensatory eye movements in goldfish (*Carassius auratus*). *J. Comp. Physiol.* 92, 37–57.
4. Harris, A.J. (1965). Eye movements of the dogfish *Squalus acanthias* L. *J. Exp. Biol.* 43, 107–138.

5. Lyon, E.P. (1900). Compensatory motions in fish. *Am. J. Physiol.* **4**, 77–82.
6. Combes, D., Le Ray, D., Lambert, F.M., Simmers, J., and Straka, H. (2008). An intrinsic feed-forward mechanism for vertebrate gaze stabilization. *Curr. Biol.* **18**, R241–R243.
7. Stehouwer, D.J. (1987). Compensatory eye movements produced during fictive swimming of a deafferented, reduced preparation *in vitro*. *Brain Res.* **410**, 264–268.
8. Azizi, E., Landberg, T., and Wassersug, R.J. (2007). Vertebral function during tadpole locomotion. *Zoology (Jena)* **110**, 290–297.
9. Hoff, K., and Wassersug, R.J. (1986). The kinematics of swimming in larvae of the clawed frog, *Xenopus laevis*. *J. Exp. Biol.* **122**, 1–12.
10. Combes, D., Merrywest, S.D., Simmers, J., and Sillar, K.T. (2004). Developmental segregation of spinal networks driving axial- and hindlimb-based locomotion in metamorphosing *Xenopus laevis*. *J. Physiol.* **559**, 17–24.
11. Straka, H., and Dieringer, N. (2004). Basic organization principles of the VOR: lessons from frogs. *Prog. Neurobiol.* **73**, 259–309.
12. Walls, G.L. (1962). The evolutionary history of eye movements. *Vision Res.* **2**, 69–80.
13. Saitoh, K., Ménard, A., and Grillner, S. (2007). Tectal control of locomotion, steering, and eye movements in lamprey. *J. Neurophysiol.* **97**, 3093–3108.
14. Lambert, F.M., Beck, J.C., Baker, R., and Straka, H. (2008). Semicircular canal size determines the developmental onset of angular vestibuloocular reflexes in larval *Xenopus*. *J. Neurosci.* **28**, 8086–8095.
15. Robinson, D.A. (1982). The use of matrices in analyzing the three-dimensional behavior of the vestibulo-ocular reflex. *Biol. Cybern.* **46**, 53–66.
16. Cochran, S.L., Kasik, P., and Precht, W. (1987). Pharmacological aspects of excitatory synaptic transmission to second-order vestibular neurons in the frog. *Synapse* **1**, 102–123.
17. Straka, H., Baker, R., and Gilland, E. (2006). Preservation of segmental hindbrain organization in adult frogs. *J. Comp. Neurol.* **494**, 228–245.
18. Pantle, C., and Dieringer, N. (1998). Spatial transformation of semicircular canal signals into abducens motor signals. A comparison between grass frogs and water frogs. *J. Comp. Physiol. A Neuroethol. Sens. Neural Behav. Physiol.* **182**, 475–487.
19. Rohregger, M., and Dieringer, N. (2002). Principles of linear and angular vestibuloocular reflex organization in the frog. *J. Neurophysiol.* **87**, 385–398.
20. Sperry, R.W. (1950). Neural basis of the spontaneous optokinetic response produced by visual inversion. *J. Comp. Physiol. Psychol.* **43**, 482–489.
21. von Holst, E., and Mittelstaedt, H. (1950). Das Refferenzprinzip. *Naturwissenschaften* **37**, 464–476.
22. Beyeler, A., Métais, C., Combes, D., Simmers, J., and Le Ray, D. (2008). Metamorphosis-induced changes in the coupling of spinal thoracolumbar motor outputs during swimming in *Xenopus laevis*. *J. Neurophysiol.* **100**, 1372–1383.
23. Dietz, V. (1992). Human neuronal control of automatic functional movements: interaction between central programs and afferent input. *Physiol. Rev.* **72**, 33–69.
24. Rudomin, P., and Schmidt, R.F. (1999). Presynaptic inhibition in the vertebrate spinal cord revisited. *Exp. Brain Res.* **129**, 1–37.
25. Shanidze, N., Kim, A.H., Loewenstein, S., Raphael, Y., and King, W.M. (2010). Eye-head coordination in the guinea pig II. Responses to self-generated (voluntary) head movements. *Exp. Brain Res.* **205**, 445–454.
26. Beisel, K.W., Wang-Lundberg, Y., Maklad, A., and Fritzsche, B. (2005). Development and evolution of the vestibular sensory apparatus of the mammalian ear. *J. Vestib. Res.* **15**, 225–241.
27. Fetcho, J.R. (1992). The spinal motor system in early vertebrates and some of its evolutionary changes. *Brain Behav. Evol.* **40**, 82–97.
28. Wada, H. (1998). Evolutionary history of free-swimming and sessile lifestyles in urochordates as deduced from 18S rDNA molecular phylogeny. *Mol. Biol. Evol.* **15**, 1189–1194.
29. Mazan, S., Jaillard, D., Baratte, B., and Janvier, P. (2000). *Otx1* gene-controlled morphogenesis of the horizontal semicircular canal and the origin of the gnathostome characteristics. *Evol. Dev.* **2**, 186–193.
30. Fritzsche, B., Signore, M., and Simeone, A. (2001). *Otx1* null mutant mice show partial segregation of sensory epithelia comparable to lamprey ears. *Dev. Genes Evol.* **211**, 388–396.
31. Lacalli, T.C. (2001). New perspectives on the evolution of protochordate sensory and locomotory systems, and the origin of brains and heads. *Philos. Trans. R. Soc. Lond. B Biol. Sci.* **356**, 1565–1572.
32. Fritzsche, B. (1996). Similarities and differences in lancelet and craniate nervous systems. *Isr. J. Zool.* **42**, 147–160.
33. Wicht, H., and Lacalli, T.C. (2005). The nervous system of amphioxus: structure, development, and evolutionary significance. *Can. J. Zool.* **83**, 122–150.
34. Brandt, T., Strupp, M., and Benson, J. (1999). You are better off running than walking with acute vestibulopathy. *Lancet* **354**, 746.
35. Brandt, T., Strupp, M., Benson, J., and Dieterich, M. (2001). Vestibulopathic gait. Walking and running. *Adv. Neurol.* **87**, 165–172.
36. Dieringer, N. (1995). 'Vestibular compensation': neural plasticity and its relations to functional recovery after labyrinthine lesions in frogs and other vertebrates. *Prog. Neurobiol.* **46**, 97–129.
37. Dietz, V. (2003). Spinal cord pattern generators for locomotion. *Clin. Neurophysiol.* **114**, 1379–1389.
38. Jahn, K., Naessl, A., Strupp, M., Schneider, E., Brandt, T., and Dieterich, M. (2003). Torsional eye movement responses to monaural and binaural galvanic vestibular stimulation: side-to-side asymmetries. *Ann. N Y Acad. Sci.* **1004**, 485–489.
39. Nieuwkoop, P., and Faber, B. (1956). *Normal Tables for Xenopus laevis* (Amsterdam: North Holland Publishing Company).